

## Very High Frame Rate Burst Image Sensors

J. K. Swain, R. Kabra, V. Patel, M. Bhaskaran,  
J. T. Andrews, P. A. Levine, and J. R. Tower  
Sarnoff Corporation, 201 Washington Road,  
Princeton, NJ 08543 [pswain@sarnoff.com](mailto:pswain@sarnoff.com)

J. L. Lowrance, V. J. Mastrocola, G. F. Renda  
Princeton Scientific Instruments  
7 Deer Park Drive, Monmouth Junction,  
NJ 08852

A family of high burst rate CCD imagers were fabricated. These imagers employ high speed, low lag photo-detectors with local storage at each photo-detector to achieve image capture at rates greater than  $10^6$  frames per second. These imagers continuously store the latest images acquired which makes it possible to capture poorly predicted and spontaneous transient events by a trigger after the event. These imagers combine a high speed, multi-implant (up to seven) pinned-buried photo-detector with local buried n-channel CCD storage elements at each macropixel. A typical cross-sectional view of the photo-detector and readout gates is shown in Figure 1. Process and device simulations were performed to optimize the potential profile of the detectors. The typical construction and operation of the photo-detector readout is shown in Figure 2. These high burst rate imagers are fabricated on p-type EPI. The new generation of CCDs employs up to four levels of polysilicon and two levels of metal. All three designs have yielded operational imagers, producing high-speed imagery in their respective camera systems. The most comprehensive data has been taken on the  $64 \times 64$  spatial resolution imager with 12 frames of storage. Table-1 summarizes the measured performance. The net quantum efficiency is the product of the fill-factor and the reported QE. Other imagers are currently under test. These cameras have been developed to capture digital image data of high-speed transient events where microsecond temporal resolution is required. Application areas include capture of rapid mechanical motion, wavefront sensing, fluid cavitation research, combustion studies, and plasma research.

**Table 1:  $64 \times 64$  Design**

Format	$64 \times 64 \times 12$ frames
Macropixel Pitch	$116 \mu\text{m} \times 116 \mu\text{m}$
Optical Fill-Factor	50%
Quantum Efficiency:	
255 nm	36%
430 nm	46%
660 nm	45%
880 nm	21%
Maximum Frame Rate	$5 \times 10^6$ fps
Full Well	30,000 e
Noise Floor	30 e RMS

Figure 1. (a) Typical cross-sectional view illustrating the photo-detector doping. (b) Corresponding potential distribution.

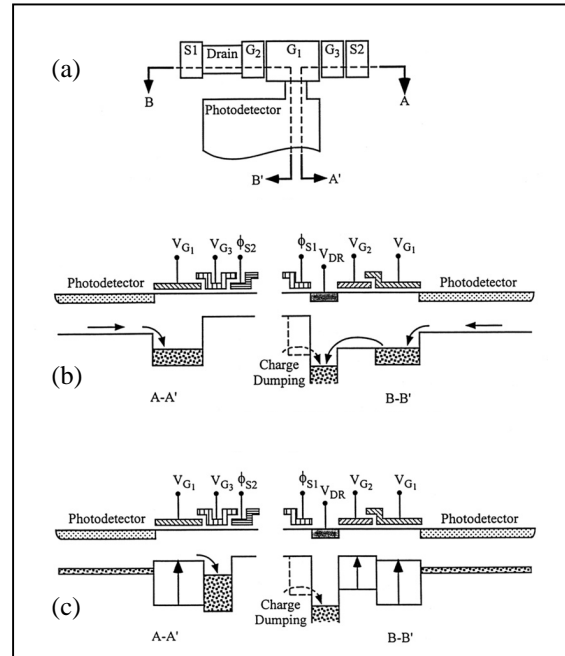


Figure 2. Typical construction and operation of photo-detector readout. (a) Top view of the photo-detector output structure. (b) Cross section of A-A' and B-B' and potential profiles during the charge accumulation. (c) Cross section of A-A' and B-B' and potential profiles during the charge readout.

